Preseismic ionospheric electron enhancements revisited

Kosuke Heki[1] and Yuji Enomoto[2]

[1]Dept. Natural History Sci., Hokkaido University, N10 W8, Kita-ku, Sapporo, Hokkaido 060-0810, Japan
[2]Toyama Industrial Technology Center, Futakami, Takaoka, Toyama 933-0981, Japan

Abstract

Possible enhancement of ionospheric Total Electron Content (TEC) immediately before the 2011 Tohoku-oki earthquake (M_w9.0) has been reported by *Heki* [2011]. Critical responses to it often come in two stages; they first doubt the enhancement itself and attribute it to an artifact. Secondly (when they accept the enhancement), they doubt the significance of the enhancement among natural variability of space weather origin. For example, *Kamogawa and Kakinami* [2013] attributed the enhancement to an artifact falsely detected by the combined effect of the highly variable TEC under active geomagnetic condition and the occurrence of a tsunamigenic ionospheric hole [*Kakinami et al.*, 2012]. Here we closely examine the time series of vertical TEC before and after the 2011 Tohoku-oki earthquake. We first demonstrate that the tsunami did not make an ionospheric hole, and next confirm the reality of the enhancement using data of two other sensors, ionosonde and magnetometers. The amplitude of the preseismic TEC enhancement is within the natural variability, and its snapshot resembles to large-scale traveling ionospheric disturbances. However, distinction could be made by examining their propagation properties. Similar TEC anomalies occurred before all the M≥8.5 earthquakes in this century, suggesting their seismic origin.

1. Introduction

Global Positioning System (GPS) receivers provide useful information on ionospheric disturbances in terms of changes in TEC, number of electrons integrated along the line-of-sight (LOS). The dense network of permanent GPS tracking stations in Japan, GEONET (GNSS Earth Observation Network), enabled in-depth studies of the ionospheric disturbances by the 2011 March 11 Tohoku-oki earthquake (M_w9.0) and its tsunami. Early papers report, e.g. fast arrival of acoustic waves at ionospheric heights [*Astafyeva et al.*, 2011], concentric wavefront by internal gravity waves [*Tsugawa et al.*, 2011], excitation of atmospheric modes [*Saito et al.*, 2011; *Rolland et al.*, 2011], and numerical simulations of these disturbances [*Matsumura et al.*, 2011]. While the majority discusses ionospheric responses to various atmospheric waves excited by the vertical movement of the ground and the sea surface, *Heki* [2011] reported possible TEC enhancement starting ~40 minutes before the earthquake. Later, *Cahyadi and Heki* [2013a, b] suggested that all the earthquakes with M_w of 8.5 or more in this century are preceded by similar preseismic TEC anomalies (except the 2005 Nias earthquake, M_w8.6, whose TEC data are disrupted by plasma bubbles).

40   Such preseismic TEC enhancements, however, have not been widely accepted in scientific communities. As a

41   typical critical response, they often doubt the existence of the TEC enhancement itself. *Heki* [2011] drew the reference

42   curves by fitting cubic polynomials to vertical TEC excluding ~1 hour period, e.g. from 40 minutes before the

43   earthquake to 20 minutes after the earthquake. However, the period to be excluded (anomalous period) is not known a-

44   priori. At a first glance, only TEC drops starting when acoustic wave disturbed the F region are clear (it takes ~10

45   minutes for acoustic waves to reach the F region of the ionosphere). Then two scenarios are possible, i.e. (1) slow

46   preseismic enhancement and its rapid recovery (Fig.1a) [*Heki*, 2011], or (2) rapid formation of an ionospheric "hole",

47   and its slow recovery (Fig.1b) [*Kakinami et al.,* 2012]. If (2) is the case, defining the reference curve by inappropriately

48   excluding the preseismic period would result in a spurious preseismic enhancement.

49   *Kakinami et al.* [2012] considered that the TEC drop after the earthquake is a phenomenon irrelevant to precursory

50   changes, and named it a tsunamigenic ionospheric hole. Typical tsunamis of interplate thrust earthquakes start with the

51   upheaval of sea surface, followed by the subsidence 5-10 minutes later. They proposed a qualitative model that

52   atmospheric waves excited by the down-going sea surface carry ionospheric electrons down and promote their

53   recombination with positive ions. Based on this concept, *Kamogawa and Kakinami* [2013] did numerical experiments

54   for daily TEC time series to demonstrate that false precursors appear by postulating such holes ~10 minutes after the

55   earthquake (as we show with the red dashed curve in Figure 1b), and concluded that the preseismic TEC enhancement

56   did not occur. Recently, *Astafyeva et al.* [2013] hypothesized that the TEC drops represent the negative phase of the

57   "N waves". In spite of different interpretation, *Kamogawa and Kakinami* [2013] and *Astafyeva et al.* [2013] are based

58   on the common idea that the TEC drops are irrelevant to precursors.

59   The present paper is partially meant to be the rebuttal to *Kamogawa and Kakinami* [2013]. We will use vertical

60   TEC (VTEC) time series on March 11, 2011 throughout this study instead of slant TEC (STEC) used in *Heki* [2011]. In

61   Section 2, we examine if the tsunami really made an ionospheric hole. In Section 3, we compare the VTEC time series

62   with data by other sensors looking for support to the preseismic TEC enhancement. In Section 4, we discuss the

63   significance of the preseismic TEC changes of the 2011 Tohoku-oki earthquake under high geomagnetic activity.

64   Finally, we discuss the implication of GPS-TEC observations for future earthquake prediction in Section 5.

65

66   **2. Does a tsunami make an ionospheric hole?**

67

68   2.1. From STEC to VTEC

69   A factor to hamper intuitive recognition of anomalous behaviors of the TEC time series obtained by GPS is the

70   existence of apparent U-shaped changes. Because GPS satellites move in the sky, changing incident angle of LOS to

71   the ionosphere causes apparent variation of STEC. Such changes can be removed by converting STEC to VTEC. Let Z

72   be the incident angle (we usually approximate the ionosphere as a thin layer at 300 km height), then STEC $\times$ cos$Z$ is the

73   VTEC. We can calculate Z from satellite orbital information.

74   To perform the conversion, we need to isolate STEC from the ionospheric (geometry-free) linear combination

75   (often called L4) of the two L-band carrier phases, L1 and L2. L4 includes integer ambiguities intrinsic to phase

measurements and inter-frequency biases (IFB) specific to transmitter (satellite) and receiver (GPS station) hardware. The first component (ambiguities) can be obtained by comparing L4 with the ionospheric combinations of the unambiguous pseudorange (code) measurements. For the Japanese GPS data, daily values of both receiver-specific IFB and satellite-specific IFB, estimated together with ionospheric models, are available online from Electronic Navigation Research Institute (ENRI) [*Sakai*, 2005]. We used them to isolate STEC from L4. Although the IFBs have some dependence on receiver temperatures [*Coster et al.*, 2013], they remain nearly constant over days. Hence, there is no technical problem in the real-time conversion from L4 to VTEC.

Figure 2 compares STEC and VTEC time series of three satellite-station pairs shown in the original article by *Heki* [2011]. Although their STEC signatures are very different, the VTEC behaves fairly similarly to each other (plot biases are given in Figure 2b to separate the curves for visual clarity). The remaining difference stems from different ionospheric penetration points (IPP). For example, because LOS to Satellite 27 has IPP in the southern sky during the first few hours, its VTEC shows somewhat higher values. IPP of Satellite 15 moves northward and then southward, resulting in a positive quadratic component which adds a gentle downward-convex curvature to the VTEC variation. Satellite 27 data before 4 UT and Satellite 26 data after 7 UT are fairly noisy because the satellite elevations are lower than 15 degrees. These parts should be excluded from further scientific discussions (also these parts represent ionosphere very far from the epicenter, see sub-ionospheric point (SIP) tracks in Figure 2c).

In Figure 2b, we can see that preseismic VTEC increases did start ~40 minutes before the mainshock (i.e. ~5 UT), and VTEC decreased to the original level after acoustic disturbances ~10 minutes after the earthquake. The VTEC curves obviously favor the "preseismic enhancement and recovery" scenario (Fig. 1a) rather than the "tsunamigenic hole formation" scenario (Fig. 1b).

Heki [2011] also pointed out that negative TEC anomalies are seen with GPS stations distant from the epicenter (see e.g. Figure A4 of *Heki* [2011] for the distribution of negative anomalies). In Figure A1, we show that VTEC of distant stations exhibit preseismic decreases. This suggests that the preseismic TEC enhancement may be a result of transportation rather than net increase of electrons.

2.2. Numerical experiments

In addition to the intuitive pattern recognition, we perform a simple numerical experiment. We will use the VTEC time series of Satellite 26 which have relatively long linearly changing portions before the earthquake. We modeled the 3 hours period encompassing the earthquake using four lines connected with three breaks (Fig.3a). Period A is assumed to represent background steady decrease of afternoon VTEC. Periods B and C correspond to the preseismic increase and coseismic decrease, respectively. Here we compare the integrated changes during B and C relative to the trend during A. If they are comparable, the extension of Period A reaches the C-D junction (as shown by broken lines in Figure 3a), i.e. there is no net VTEC decrease.

The results in Figure 3c suggest that the two quantities are identical within errors. Hence, the coseismic decrease is interpreted as the recovery from the preseismic increase. Because the tsunami did not create a hole in an active sense, the word "tsunamigenic ionospheric hole" might be misleading. The process hypothesized by *Kakinami et al.* [2012]

112 may have worked in a short timescale, i.e. down-going sea surface resulted in the decrease of ionospheric electrons.

113 However, it is not a stand-alone phenomenon but a part of a longer process. We conclude that the artifact claim for the

114 2011 Tohoku-oki and the 2010 Maule cases by *Kamogawa and Kakinami* [2013] is not substantiated because it is based

115 on the existence of the tsunamigenic ionospheric hole without preseismic changes.

116   VTEC in Period D shows wavy postseismic behaviors. Some stations (e.g. 0572) show increase while other stations

117 (e.g. 0265) do not. The positive VTEC anomalies around the end of the Period D correspond to the crest of a concentric

118 wavefront around the "ionospheric" epicenter. The geographical distribution of these anomalies at this time epoch (i.e.

119 06:25 UT) is available in the Figure 2f of *Tsugawa et al.* [2011].

120

121 **3. Do other sensors show preseismic changes?**

122

123 3.1. Three sensors in the same time window

124   If the preseismic TEC anomaly involved transportation of electric charges in the ground and/or ionosphere, it should

125 have accompanied electric currents and consequent changes in the geomagnetic field. *Utada et al.* [2011] showed co-

126 and postseismic geomagnetic field changes of the 2011 Tohoku-oki earthquake and its tsunami. Although they did not

127 pay attention to changes before the earthquake, *Enomoto* [2012] pointed out that the geomagnetic anomalies of several

128 nT associated with the 2011 Tohoku-oki earthquake were observable at stations in NE Japan. In fact, geomagnetic

129 declination in *Utada et al.* [2011] showed gradual changes up to 1 arc minute starting ~40 minutes before the

130 earthquake. We downloaded geomagnetic data archive from Japan Meteorological Agency (JMA), and plot the

131 declination change at Kakioka (KAK), Kanto, relative to Kanoya (KNY) in Kyushu, in Figure 4.

132   Ionosonde observations are done at four stations in Japan, in which Kokubunji, west of Tokyo, is the nearest to the

133 2011 Tohoku-oki rupture area. Peak plasma frequencies at Kokubunji are available from the World Data Center for

134 Ionosphere (WDC) (wdc.nict.go.jp). The F2 peak plasma frequency (foF2) remained high over the few days before the

135 2011 Tohoku-oki earthquake, but did not show significant changes immediately before and after the earthquake.

136 However, the critical frequency at the sporadic-E (Es) layer (foEs) showed sudden appearance of the reflection at 5:30

137 UT, and it lasted until 6:15 UT (Fig.4). The Es occurrence is controlled by neutral wind shear rather than space weather

138 [e.g. *Whitehead*, 1989], and there were no enhanced Es activities at this time. The foEs at 5:30 implies only moderate

139 increase of electron density in the E region, but it is the highest in this week (days 067-073) (Fig.A2). Similar

140 discussion on the foF2 and foEs behaviors is to be found in *Carter et al.* [2013].

141   Figure 4 compares the time series of the two new observables in addition to VTEC (Satellite 15 at 3009). Both of

142 the VTEC and the declination residual show moderate anomalies starting ~40 minutes before the 2011 Tohoku-oki

143 earthquake, and disappear after the earthquake. Although the foEs time resolution is 15 minutes, its first appearance at

144 5:30 UT is consistent with the other two. As a whole, Figure 4 would give a certain support to the reality of the

145 preseismic TEC enhancement.

146   The foEs data suggested the electron density increase in the E region rather than the F region. This is consistent with

147 the electron density profile above the Tohoku District (position shown in Figure 4b) from the COSMIC-2

148   (Constellation Observing System for Meteorology, Ionosphere, and Climate) GPS radio occultation measurements at

149   5:50 UT (4 minutes after the earthquake). The actual profile shown in *Astafyeva et al.* [2011] indicates that electrons in

150   the E region was >3 times as dense as the IRI-2007 model [*Bilitza and Reinisch*, 2008] while little anomalies are seen

151   in the F region. The electron density increase in the E region may better explain the TEC decrease after the acoustic

152   disturbance (called "tsunamigenic ionospheric hole" by them), i.e. the recombination process proposed by *Kakinami et*

153   *al.* [2012] may work more efficiently for lower altitude electrons.

154

155   3.2. Geomagnetic declination

156   Geomagnetic data at seven observatories are available on the web, i.e. four Japan Meteorological Agency (JMA)

157   stations at Memanbetsu (MMB), Hokkaido, Kakioka (KAK), Kanto, Kanoya (KNY), Kyushu, and Chichijima (CBI),

158   the Bonin Islands, and three Geospatial Information Authority of Japan (GSI) stations at Esashi (ESA) and Mizusawsa

159   (MIZ), Tohoku, and Kanozan (KNZ), Kanto. In Figure 5, we show time series of the geomagnetic declination at six

160   stations with respect to KNY. On the earthquake day (Fig.5b), stations close to the epicenter showed preseismic

161   declination changes. The anomalies at ESA, MIZ, KAK, KNZ seem to have started simultaneously at ~40 minutes

162   before the earthquake, the same onset time as the VTEC anomaly. Such an anomaly is not seen at CBI, and is vague at

163   MMB. Preseismic anomalies are not clear in other components (e.g. intensity of horizontal and vertical components,

164   see Figure A3), suggesting that the disturbing field was dominantly east-west.

165

166

167   **4. Is the preseismic TEC change significant?**

168

169   We do not claim that any of the VTEC, geomagnetic declination, and foEs exceeded normal variability under active

170   geomagnetic conditions. Indeed, space weather directly influences these quantities. On the other hand, an earthquake is

171   a phenomenon to release lithospheric stress, and could influence the upper atmosphere and geomagnetism only

172   indirectly. The 2011 Tohoku-oki earthquake was an unprecedented M9-class earthquake with recurrence interval

173   exceeding five centuries. However, one should never expect this earthquake to produce "unprecedented" anomalies in

174   the ionosphere and geomagnetic fields.

175   Figure 6a shows the auroral electrojet (AE) index and the geomagnetic activity indices Kp and Dst over three weeks

176   from day 053 (Feb.22) to 074 (Mar. 15). Geomagnetic condition was calm only in the first week, and the second/third

177   weeks include lots of minor disturbances including the geomagnetic storm on Mar. 1 (day 060). Relatively strong

178   geomagnetic disturbance took place also on the day of the earthquake (day 070); Dst reached minimum shortly before

179   the earthquake and the AE index showed related substorm activities. As pointed out by *Carter et al.* [2013], the

180   ionosphere is likely to be highly variable before and after the earthquake, making it difficult to identify preseismic

181   anomalies confidently.

182   Figure 6b-d shows VTEC of Satellite 15 at 3009 over this period. The four-hour time window was shifted by 0.5

183   hours per week because GPS satellites rise ~4 minutes earlier every day. VTEC variability faithfully reflects

184 geomagnetic activities, i.e. it shows simple decreases during the first week while its day-to-day variability is two- or
185 threefold in the last two weeks. The preseismic anomaly in question (day 070) may exceed the natural variability of the
186 quiet week, but the natural variability of the later weeks overwhelms the anomaly.

187   A number of small VTEC disturbances during the week 2 and 3 are understood as the passages of small amplitude
188 LSTIDs (large-scale travelling ionospheric disturbance) propagating southward from the auroral oval as atmospheric
189 gravity waves. In Figure 7, we show VTEC time series by Satellite 15 at eight coastal GPS stations from Hokkaido to
190 the Kanto District with approximate separation of ~200 km. There, we can identify two kinds of VTEC disturbances,
191 the first one is a small negative anomaly appearing around ~4.5 UT at the northernmost station, and the second one is
192 the possible precursory enhancement. The second one is stationary and appears to have started simultaneously ~40
193 minutes before the earthquake. The first one, on the other hand, traveled southward with an approximate speed of 0.3
194 km/s. In Figure A4, we show that two small-scale irregularities seen on days 068 and 072 (Fig. 6d) are also LSTIDs
195 propagating southward. The geomagnetic declination residual time series at KAK over seven consecutive days (Fig.
196 5a) show that it also suffers from natural variability due to space weather.

197
198

199 **5. Discussion and conclusion**

200

201 5.1. Repeatability for past $M_w \geq 8.5$ earthquakes

202   In Section 2, we demonstrated that the VTEC data before and after the 2011 Tohoku-oki earthquake do not support
203 the tsunamigenic ionospheric hole hypothesis (Fig. 1b) [*Kakinami et al.,* 2012], but favored the preseismic increase and
204 recovery scenario (Fig.1a). In Section 3, we showed that two additional sensors, ionosonde and magnetometer, showed
205 simultaneous anomalies. Considering these points, we concluded that the ionospheric electron enhancement did start
206 ~40 minutes before the earthquake. In Section 4, however, we showed that this earthquake occurred during a period of
207 high geomagnetic activity, and the observed preseismic anomalies did not exceed non-seismic natural variability. There
208 we showed that the preseismic changes could be distinguished from LSTID by monitoring their propagation.
209 Nevertheless, it would be fair to say that we cannot prove this particular preseismic TEC enhancement to be an
210 earthquake precursor.

211   Acoustic waves excited by coseismic vertical crustal movements disturb the ionosphere ~10 minutes after
212 earthquakes. Such coseismic ionospheric disturbances have been detected by GPS networks for >20 earthquakes [e.g.
213 *Astafyeva et al.,* 2013; *Cahyadi and Heki*, 2013b]. Although their amplitudes are less than non-seismic natural
214 variability in most cases, their existence has never been questioned. That is because (1) they have spatial and temporal
215 correlation with earthquakes (e.g. the spatial pattern of wavefront, delayed emergence with a time lag of ~10 minutes),
216 and (2) its physical mechanisms are understood. As for the preseismic TEC enhancement, its physical mechanism is yet
217 to be clarified, but it certainly has characteristics to suggest its earthquake origin, i.e. high repeatability for large
218 earthquakes.

219   From the VTEC time series before and after the 2011 Tohoku-oki earthquake, we found that earthquake-related
220   ionospheric disturbances start ~40 minutes before the earthquake and end shortly after the acoustic disturbance. Let us
221   assume that this emergence time window is common for other large earthquakes, i.e. we could isolate earthquake-
222   related TEC signals by fitting reference curves to VTEC using a polynomial (degree 1-3 depending on the arc lengths
223   and TEC variability) excluding the one-hour period (from -40 minutes to +20 minutes relative to earthquakes). Then,
224   all the earthquakes in the 21st century with $M_w \geq 8.5$ (six in total) show similar preseismic TEC enhancements. *Heki*
225   [2011] showed it for the 2004 Sumatra-Andaman (M_w9.2) and 2010 Maule (M_w8.8) earthquakes as well as for the 2011
226   Tohoku-oki earthquake (M_w9.0). Later, we found it for the 2007 Bengkulu earthquake (M_w8.5) and the 2012 M_w8.6
227   strike-slip earthquake (including its M_w8.2 aftershock) off the Indian Ocean coast of Northern Sumatra [*Cahyadi and*
228   *Heki*, 2013a, b]. So far, only one exception is the 2005 Nias earthquake (M_w8.6), for which daily repeating plasma
229   bubble activities hid all earthquake-related TEC signatures [*Cahyadi and Heki*, 2013a].
230   After all, the problem will be a matter of probability. In Figure 8, we compare the VTEC residuals of the 2011
231   earthquake with those for the three earthquakes not covered in the first paper [*Heki*, 2011], the 2007 Bengkulu
232   earthquake [*Cahyadi and Heki*, 2013a], the 2012 North Sumatra earthquake, and its largest aftershock (M_w8.2) that
233   occurred ~2 hours later [*Cahyadi and Heki*, 2013b]. There, the reference curves were defined by fitting the VTEC
234   before and after the earthquake excluding one-hour period using degree 1-3 polynomials. They show striking
235   similarities, steady growth after the onset ~40 minutes before earthquakes and quick recovery after acoustic
236   disturbances. In order to rule out the seismic origin of these anomalies, we will have to attribute all these similar
237   anomalies to space weather. To us, this seems very unlikely.
238   Let us assume a certain probability that similar TEC enhancements appear immediately before $M_w \geq 8.5$ earthquakes
239   by chance (i.e. the probability that an LSTID happen to pass over the rupture area immediately before an earthquake by
240   chance). Even if this probability is as large as 1/3, the probability that the same anomalies occur for all the five $M_w \geq 8.5$
241   earthquakes (those in 2004, 2007, 2010, 2011, 2012) is $(1/3)^5$, i.e. <0.5 percent. Geomagnetic activities were fairly calm
242   before and after the 2007 and 2010 earthquakes, and the actual possibility would be much smaller than 1/3. This is why
243   we think that the TEC enhancements observed before $M_w \geq 8.5$ earthquakes are their precursors in spite of their
244   amplitudes smaller than non-seismic natural variability.
245   By the way, we have studied ionospheric disturbances of five $8.5 > M_w \geq 8.0$ events with regional GPS networks
246   available. We found immediate preseismic TEC anomalies for the two, i.e. the 1994 Hokkaido-Toho-Oki earthquake
247   (M_w8.3) [*Heki*, 2011] and the largest aftershock of the 2012 North Sumatra earthquake (M_w8.2) [*Cahyadi and Heki*,
248   2013b], but not for the other three (the 2003 Tokachi-oki, the 2006 Kuril thrust, and the 2007 Kuril outer rise
249   earthquakes). There have been no preseismic TEC anomalies found so far for earthquakes with M_w below 8.

250

251   5.2. Implication for earthquake prediction
252   Here we discuss if the preseismic TEC enhancement satisfies the four requirements in the "guideline for submission
253   of earthquake precursor candidates" by *Wyss* [1991]. The validation criteria require that the observed anomaly (a)
254   should have a relation to stress, strain, or some mechanism leading to earthquakes, (b) should be simultaneously

observed on more than one instruments, or at more than one site, and (c) the amplitude of the anomaly should bear a relation to the distance from the eventual mainshock, and (d) the ratio of the size (in space and time) of the dangerous zone to the total region monitored shall be discussed to evaluate the usefulness.

The TEC enhancement would clear (b)-(d), but (a) remains unclear. The multi-sensor observations indicate that the phenomenon that started ~40 minutes before the earthquake should accompany (1) TEC enhancement (and possibly decrease in the area relatively far from the epicenter, see Figure A1), (2) electron density increase in the E region of the ionosphere, (3) geomagnetic declination changes, and (4) quick disappearance after acoustic disturbances. They would certainly narrow the candidates of the physical processes. *Enomoto* [2012] proposed coupled interaction of earthquake nucleation with deep earth gases, and induced electric currents in the sea water and magnetic field in ionosphere as a possible mechanism for seismo-electromagnetic precursors including the TEC enhancement.

Feasibility of the practical earthquake prediction by monitoring TEC is not clear. Rapid recognition of arrivals of LSTID that propagated from the auroral oval would be crucial to distinguish preseismic TEC disturbances out of non-seismic disturbances during high geomagnetic activity. Once its physical mechanism is identified, the most appropriate sensors should be sought in addition to GPS-TEC toward operational earthquake prediction in the future.

5.3. Conclusions

This study can be concluded as follows,

(1) VTEC plot is useful to intuitively understand what is happening in the ionosphere.

(2) The 2011 Tohoku-oki earthquake tsunami did not cause net decrease of TEC.

(3) VTEC, geomagnetic declination, and foEs started to change simultaneously ~40 minutes before the 2011 Tohoku-oki earthquake.

(4) Observed preseismic anomalies do not exceed natural variability under high geomagnetic activity. Typical non-seismic variations are small amplitude LSTIDs and could be distinguished by detecting their southward propagation.

(5) Repeatability of the TEC enhancement immediately before $M_w \geq 8.5$ earthquakes suggests its seismic origin.

(6) Further investigation of its physical mechanism should be pursued.

References

Astafyeva, E., P. Lognonné, and L. Rolland (2011), First ionospheric images of the seismic fault slip on the example of the Tohoku-oki earthquake, *Geophys. Res. Lett., 38*, L22104, doi:10.1029/2011GL049623.

292 Astafyeva, E., S. Shalimov, E. Olshanskaya, and P. Lognonné (2013), Ionospheric response to earthquakes of different

293   magnitudes: Larger quakes perturb the ionosphere stronger and longer, *Geophys. Res. Lett., 40*, 1675-1681,

294   doi:10.1002/grl.50398.

295 Bilitza, D. and B. Reinisch (2008), International Reference Ionosphere 2007: Improvements and new parameters, *Adv.*

296   *Space Res., 42 (4)*, 599-609, doi:10.1016/j.asr.2007.07.048.

297 Cahyadi, M. N. and K. Heki (2013a). Ionospheric disturbances of the 2007 Bengkulu and the 2005 Nias earthquakes,

298   Sumatra, observed with a regional GPS network. *J. Geophys. Res., 118,* 1-11, doi:10.1002/jgra.50208.

299 Cahyadi, M. N. and K. Heki (2013b), Coseismic ionospheric disturbance of the 2012 North Sumatra earthquakes, large

300   intra-plate strike-slip events, *J. Geophys. Res. Space Phys.*, submitted.

301 Carter, B. A., A. C. Kellerman, T. A. Kane, P. L. Dyson, R. Norman, and K. Zhang (2013), Ionspheric precursors to

302   large earthquakes: A case study of the 2011 Japanese Tohoku Earthquake, *J. Atmos. Solar-Terr. Phys., 102*, 290-

303   297, doi:10.1016/j.jastp.2013.06.006.

304 Coster, A., J. Williams, A. Weatherwax, W. Rideout, and D. Herne (2013), Accuracy of GPS total electron content:

305   GPS receiver bias temperature dependence, *Radio Sci., 48*, 190-196, doi:10.1002/rds.200011.

306 Enomoto, Y. (2012), Coupled interaction of earthquake nucleation with deep earth gases: a possible mechanism for

307   seismo-electromagnetic phenomena, *Geophys. J. Int., 191*, 1210-1214, doi:10.1111/j.1365-246X.2012.05702.x.

308 Heki, K. (2011), Ionospheric electron enhancement preceding the 2011 Tohoku-Oki earthquake, *Geophys. Res. Lett. 38*,

309   L17312, doi:10.1029/2011GL047908.

310 Kakinami, Y., M. Kamogawa, Y. Tanioka, S. Watanabe, A. R. Gusman, J.-Y. Liu, Y. Watanabe, and T. Mogi (2012),

311   Tsunamigenic ionospheric hole, *Geophys. Res. Lett. 39*, L00G27, doi:10.1029/2011GL050159.

312 Kamogawa, M. and Y. Kakinami (2013), Is an ionospheric electron enhancement preceding the 2011 Tohoku-oki

313   earthquake a precursor?, *J. Geophys. Res., 118*, 1-4, doi:10.1002/jgra.50118.

314 Matsumura, M., A. Saito, T. Iyemori, H. Shinagawa, T. Tsugawa, Y. Otsuka, M. Nishioka, and C.H. Chen (2011),

315   Numerical simulations of atmospheric waves excited by the 2011 off-the-Pacific coast of Tohoku Earthquake, *Earth*

316   *Planets Space, 63*, 885-889.

317 Rolland, L. M., P. Lognonné, E. Astafyeva, E. A. Kherani, N. Kobayashi, M. Mann, and H. Munekane (2011), The

318   resonant response of the ionosphere imaged after the 2011 off-the-Pacific coast of Tohoku Earthquake, *Earth*

319   *Planets Space, 63*, 853-857.

320 Saito, A., T. Tsugawa, Y. Otsuka, M. Nishioka, T. Iyemori, M. Matsumura, S. Saito, C.H. Chen, Y. Goi, and N.

321   Choosakul (2011), Acoustic resonance and plasma depletion detected by GPS total electron content observation

322   after the 2011 off-the-Pacific coast of Tohoku Earthquake, *Earth Planets Space, 63*, 863-867.

323 Sakai, T. (2005), Bias error calibration for observing ionosphere by GPS network, *J. Inst. Electronics Info. Comm. Eng.,*

324   *J88-B*, 2382-2389 (in Japanese).

325 Tsugawa, T., A. Saito, Y. Otsuka, M. Nishioka, T. Maruyama, H. Kato, T. Nagatsuma, and K.T. Murata (2011),

326   Ionospheric disturbances detected by GPS total electron content observation after the 2011 off-the-Pacific coast of

327   Tohoku Earthquake, *Earth Planets Space, 63*, 875-879.

328   Utada, H., H. Shimizu, T. Ogawa, T. Maeda, T. Furumura, T. Yamamoto, N. Yamazaki, Y. Yoshitake, and S.
329   Nagamachi (2011), Geomagnetic field changes in response to the 2011 off the Pacific Coast of Tohoku earthquake
330   and tsunami, *Earth Planet. Sci. Lett., 311*, 11-27, doi:10.1016/j.epsl.2011.09.036.
331   Whitehead, J. D. (1989), Recent work on mid-latitude and equatorial sporadic-E, *J. Atmos. Terr. Phys., 51*, 401-424.
332   Wyss, M. (Ed.) (1991), Evaluation of proposed earthquake precursors, pp. 94, American Geophysical Union,
333   Washington D.C., doi:10.1029/SP032.

334
335
336   **Figures**
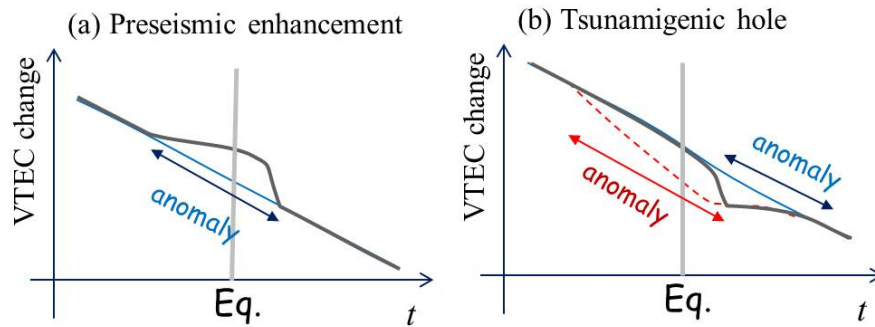
337
338
339   Figure 1. Two concepts to explain TEC drops occurring ~10 minutes after the earthquake, i.e. (a) slow preseismic TEC
340   enhancement and its recovery [*Heki*, 2011] and (b) tsunamigenic hole formation and its slow recovery [*Kakinami et
341   al.*, 2012]. Curves in light blue are the reference, and anomaly is defined as the departure from the reference curves.
342   The two scenarios agree with the existence of the TEC drop ~10 minutes after the earthquake. However, the scenario
343   (b) considers that there were no preseismic anomalies and the spurious preseismic anomaly would emerge if we
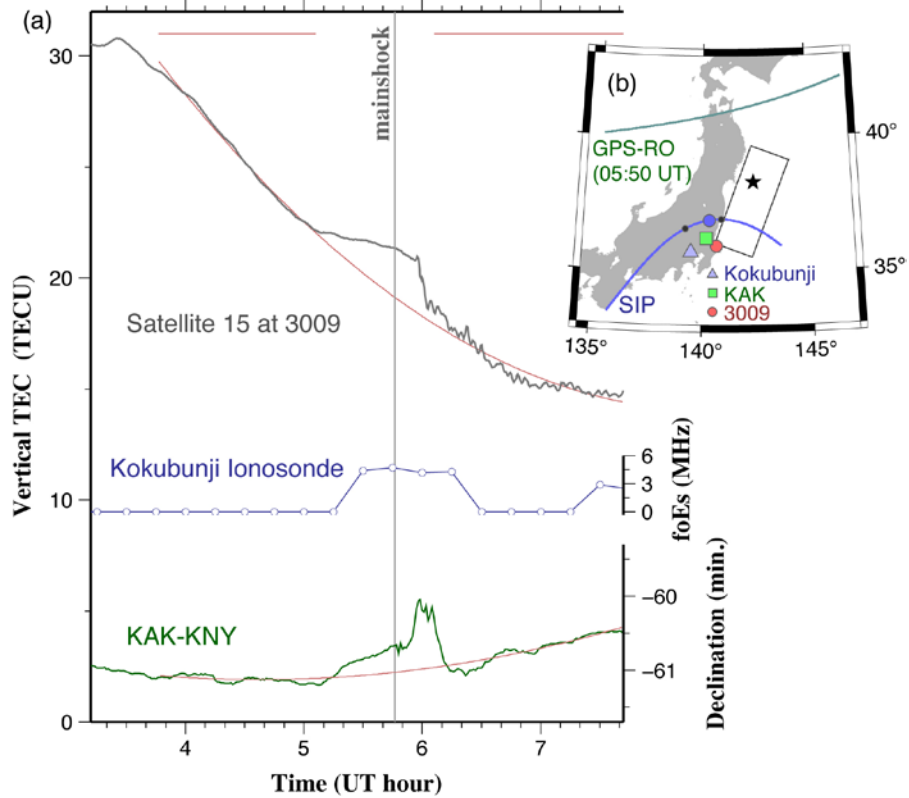344   define the reference curve inappropriately (dashed curve in red).

345
346
347
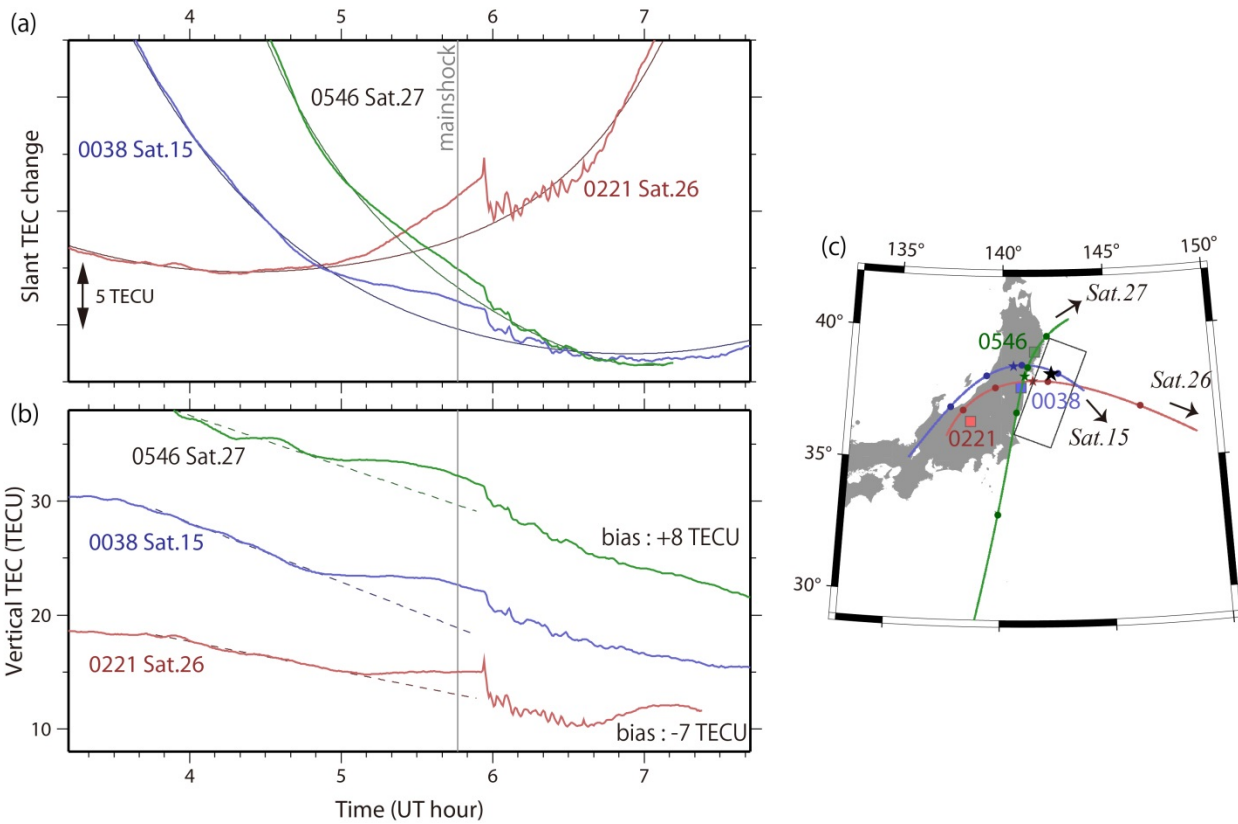
348
349 Figure 2. Time series of STEC changes (a) and VTEC (b) of Satellites 15 (blue), 26 (red) and 27 (green) observed at
350 0038, 0221 and 0546, respectively. The reference smooth curves in (a) were obtained following *Heki* [2011]. In the
351 VTEC plot, the portions 1-2 hours before the mainshock were modeled with lines and extrapolated to the earthquake
352 occurrence time (dashed lines in b). SIP trajectories of the three satellites are plotted using the same color in (c).
353 Stars on the SIP tracks show SIP positions at 5.77 UT (mainshock time), and circles on the SIP tracks are 1 hour time
354 marks. The rectangle and the black star show the approximate fault area and the epicenter of the 2011 Tohoku-oki
355 earthquake.
356
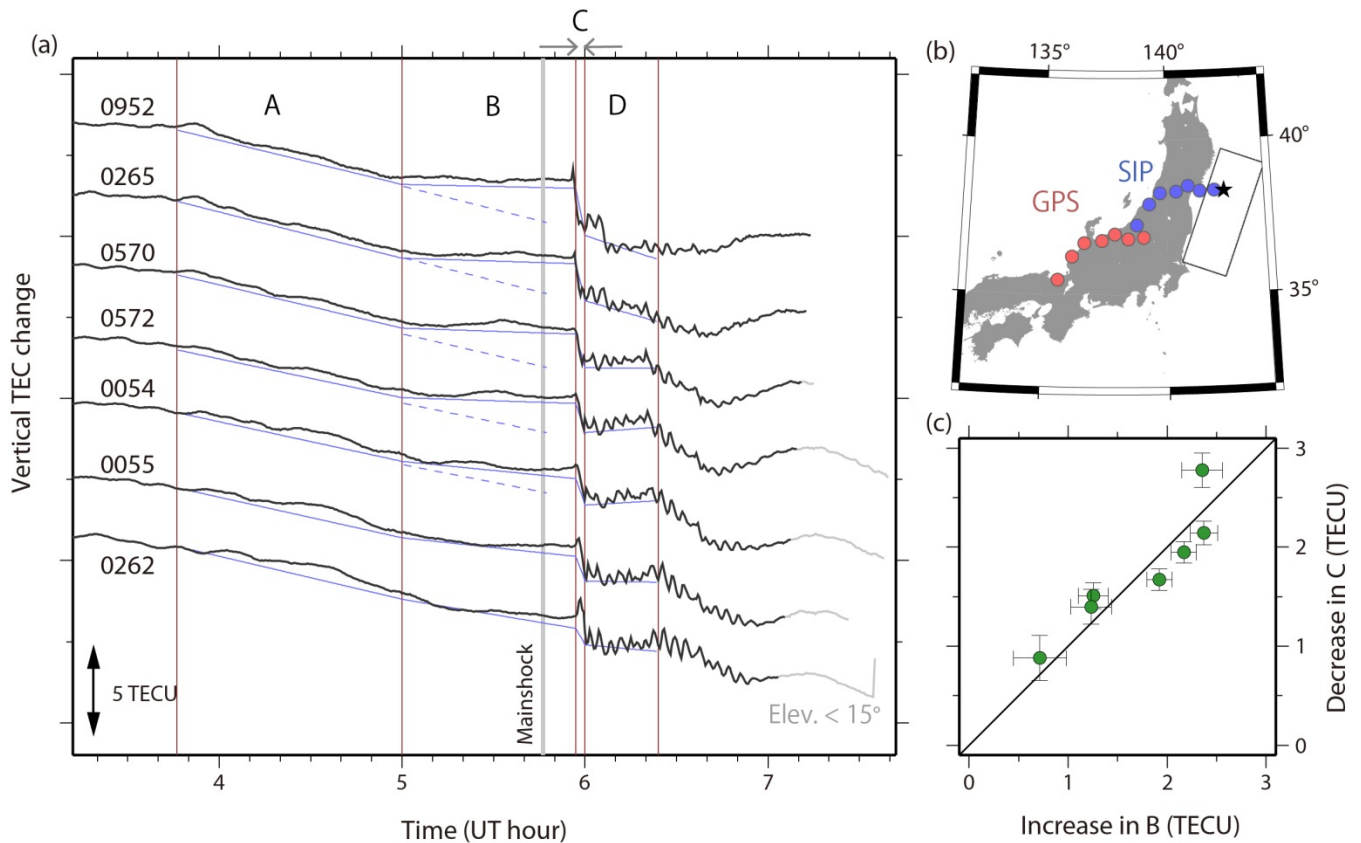
357
358
359   Figure 3. (a) Satellite 26 VTEC time series at 7 GPS stations with various focal distances. Parts shown with light gray
360   indicate the data obtained with satellite elevations lower than 15 degrees. We divided ~3 hour period from 3.77 UT (2
361   hours before the earthquake) to 6.4 UT (~40 minutes after the earthquake) into four portions representing (A) normal
362   background, (B) precursory enhancement, (C) coseismic drop, and (D) postseismic period, and fit lines with three
363   breaks. In (b) we show GPS stations and their SIP at 5:46 UT. Their preseismic increases (increase during B relative
364   to the trend in A) are compared with the decrease during C (error bars show 1σ) (c).
365
366

Figure 4. Comparison of signals by the three sensors, VTEC by Satellite 15 at the station 3009 (grey curve), E layer critical frequency (foEs) from the ionosonde at Kokubunji (blue curve), and the geomagnetic field declination at KAK, Kanto, relative to KNY, Kyushu (green curve) (a). The anomalies show up simultaneously ~40 minutes before the 2011 Tohoku-oki earthquake. Reference quadratic curves for VTEC and the geomagnetic declination have been drawn by fitting the part shown by horizontal lines at the top. Positions of the observatories are shown in (b). Black dots on the SIP trajectory show the positions at 5 and 6 UT. The dark green curve in (b) shows the IPP track of the GPS Radio Occultation measurement at 5:50 UT shown in *Astafyeva et al.* [2011]
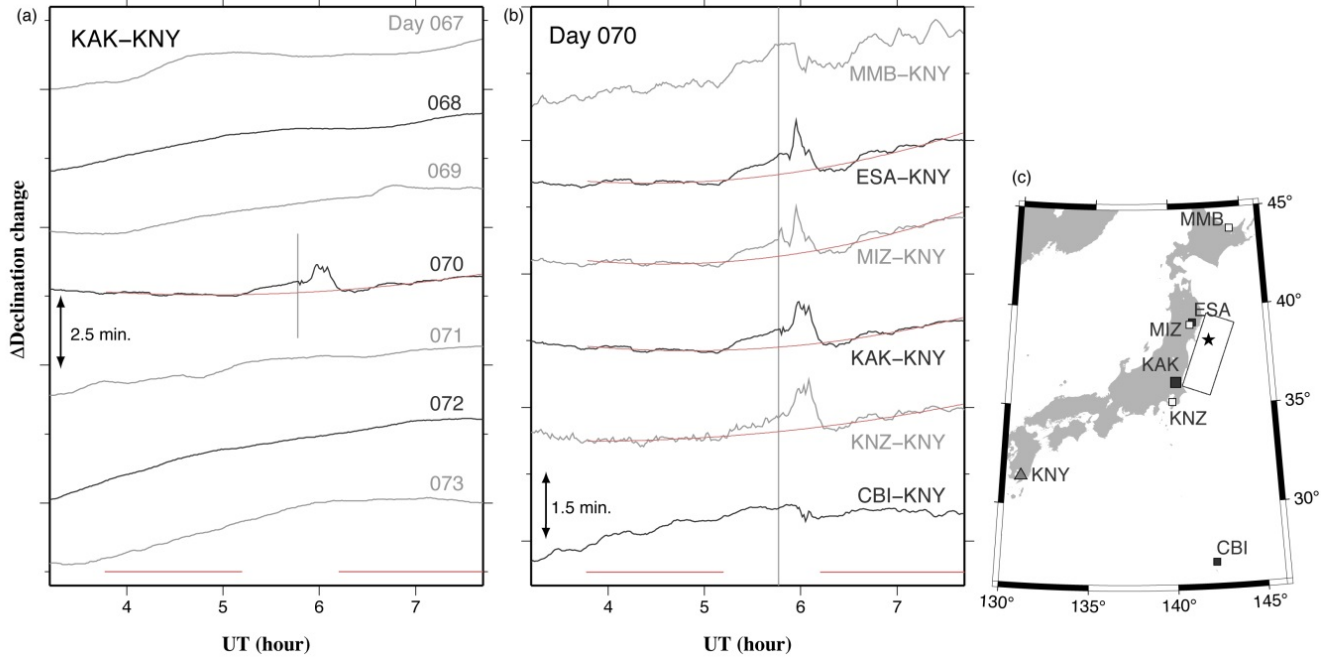
Figure 5. (a) Geomagnetic declination at Kakioka (KAK) relative to Kanoya (KNY) over the seven days period encompassing the earthquake day (070). In (b), the declination changes relative to KNY of six geomagnetic observatories in Japan (c) on the earthquake day are shown. Model fitting with quadratic functions, similar to Figure 4, has been done for the data on the earthquake day (red curves). Positive anomalies are seen to have started ~40 minutes before the 2011 Tohoku-oki earthquake for stations in the Tohoku and the Kanto District. Vertical lines in (a) and (b) indicate the earthquake occurrence time.
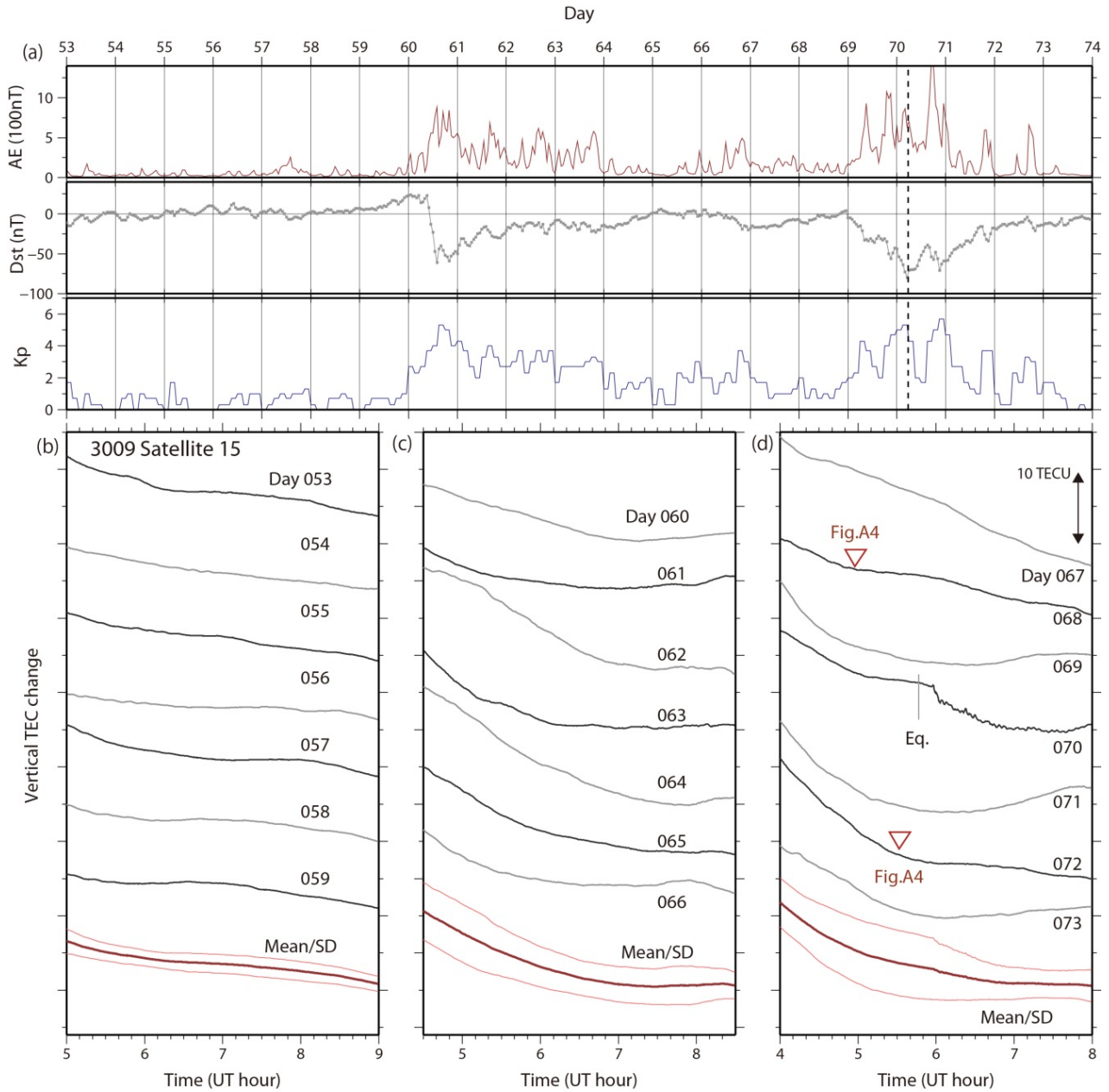
386
387
388 Figure 6. Auroral electrojet (AE), and Dst/Kp indices over the three weeks period from day 053 to day 073 in 2011
389   show high geomagnetic activity in the second and the third weeks (a). The VTEC time series at the GPS station 3009
390   with Satellite 15 over 4-hour period show gentle afternoon decrease in the first week (b), but complicated behaviors
391   arise in the next two weeks (c,d). The two rather sharp bends on the days 068 and 072 are shown to be LSTID origin
392   in Figure A4. The weekly mean VTEC and 1σ standard deviations are given at the bottom.
393
394
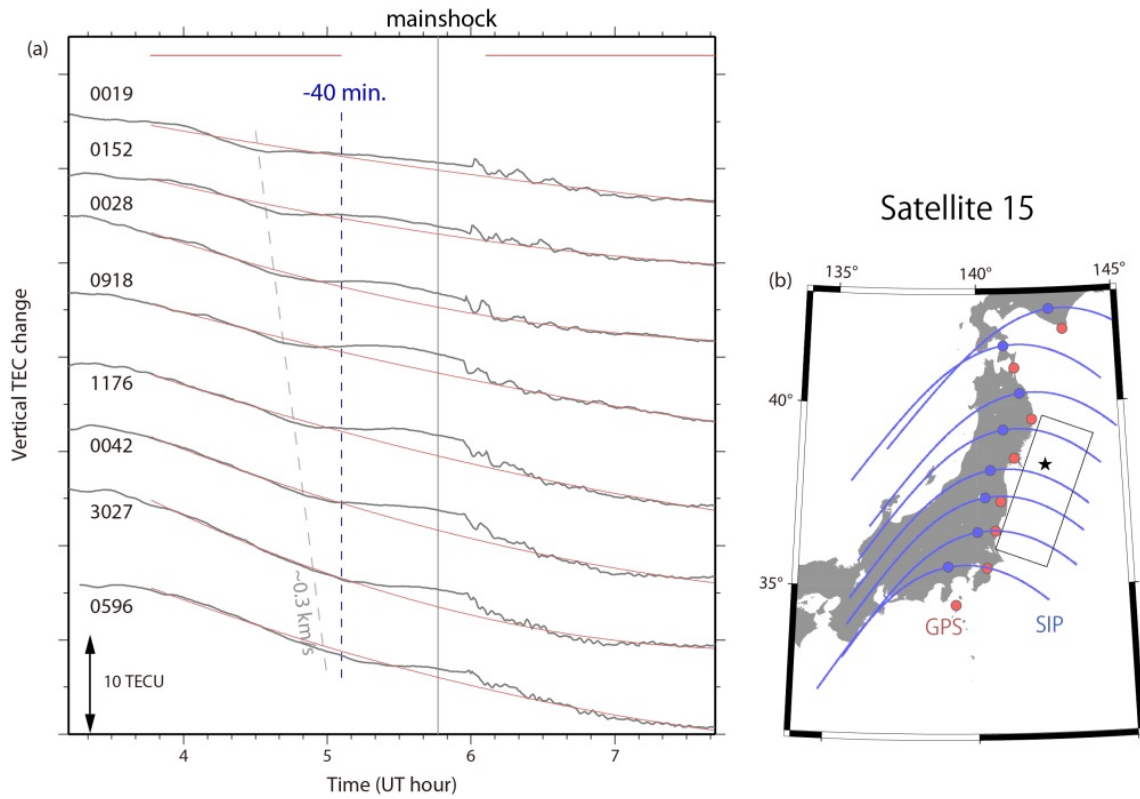
395
396 Figure 7. VTEC time series by Satellite 15 (a) at 8 GPS stations shown in (b). Reference curves in red were drawn by
397 fitting the parts shown by the horizontal red lines at the top using quadratic functions. SIP trajectories are shown by
398 blue curves in (b). A positive VTEC anomaly seems to have started simultaneously ~40 minutes before the
399 earthquake (vertical broken line). In addition to that, a small negative anomaly, possibly a small-amplitude LSTID,
400 propagate from north to south by ~0.3 km/sec.
401
402
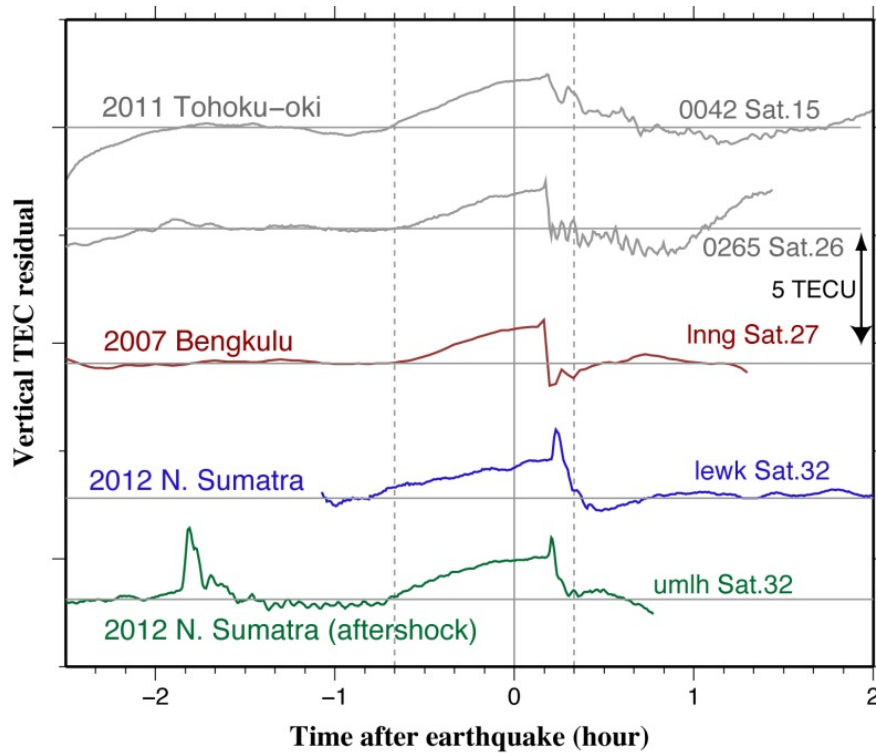
Figure 8. VTEC residuals from reference polynomials estimated excluding the period between the two broken lines (from -40 to +20 minutes) for the 2011 Tohoku-oki earthquake and three other earthquakes, i.e. the 2007 Bengkulu earthquake (M_w8.5), 2012 North Sumatra earthquake (M_w8.6), and its largest aftershock (M_w8.2) that occurred ~2 hours later. Polynomial degrees are 2, 1, 3, 3, 2 from top to bottom. See *Cahyadi and Heki* [2013a,b] for the details of the data of the 2007 and 2012 earthquakes. The GPS station names and the satellite numbers are shown to the right. A strong positive anomaly seen in the bottom curve about -1.8 hours is the coseismic ionospheric disturbance of the main shock.

415   Auxiliary Materials
416
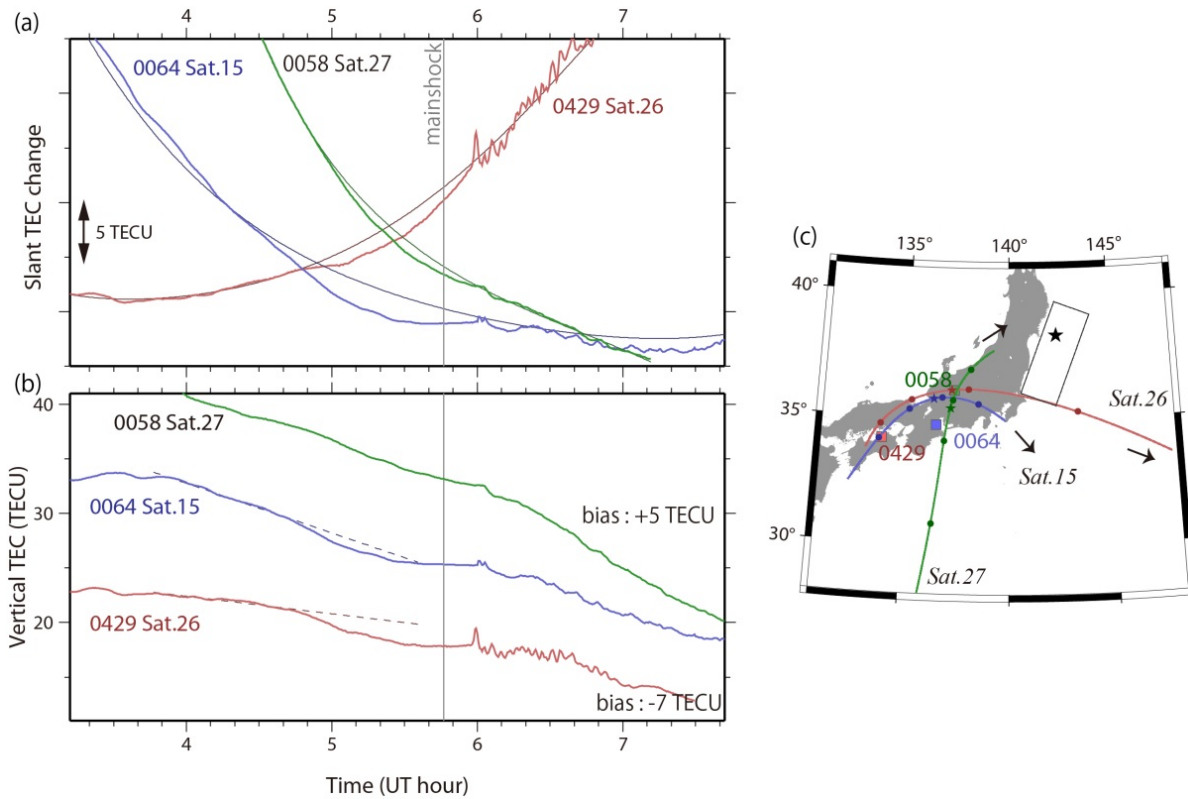
417
418
419   Figure A1. Time series of STEC changes (a) and VTEC (b) of Satellites 15 (blue), 26 (red) and 27 (green) observed at
420   0064, 0429 and 0058, respectively. See the caption of Figure 2 for the detail. These data represent ionosphere
421   relatively far from the epicenter, and VTEC shows slight decrease before the earthquake.
422
423
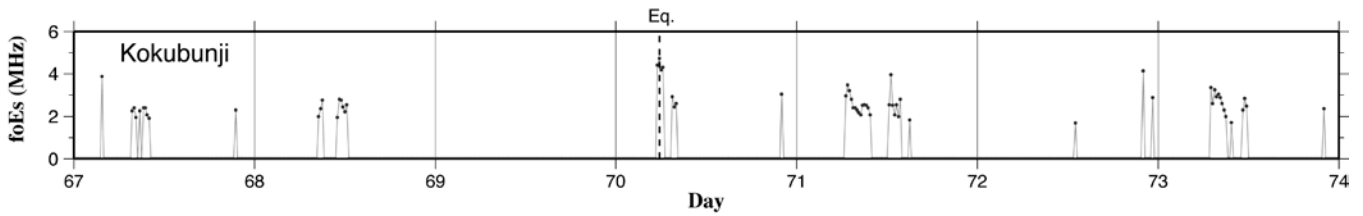
424
425
426   Figure A2. foEs at the Kokubunji ionosonde (Fig.4b) over the days 067-073. Although relatively high foEs is seen on
427   the earthquake day (day 070), similar enhancements are seen from time to time.
428
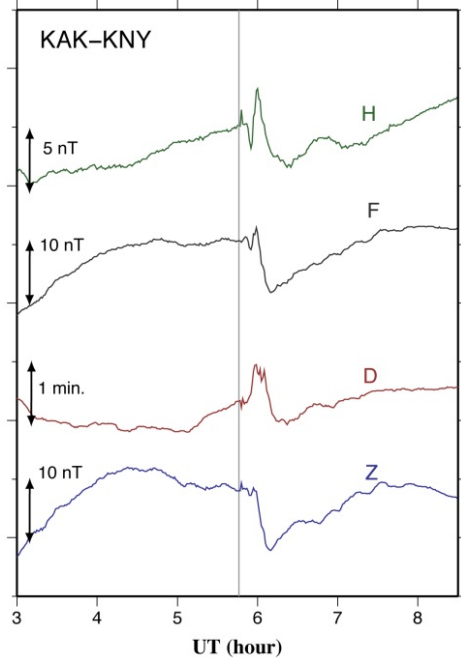
429
430
431 Figure A3. Time series of the horizontal component (H), total force (F), declination (D), and the vertical component (Z)
432 of the geomagnetic fields of KAK relative to KNY. Change starting at ~40 minutes before the earthquake is clear
433 only in D, suggesting that the additional magnetic field is approximately in east-west direction. See Figure 5b for the
434 observatory positions.
435
436
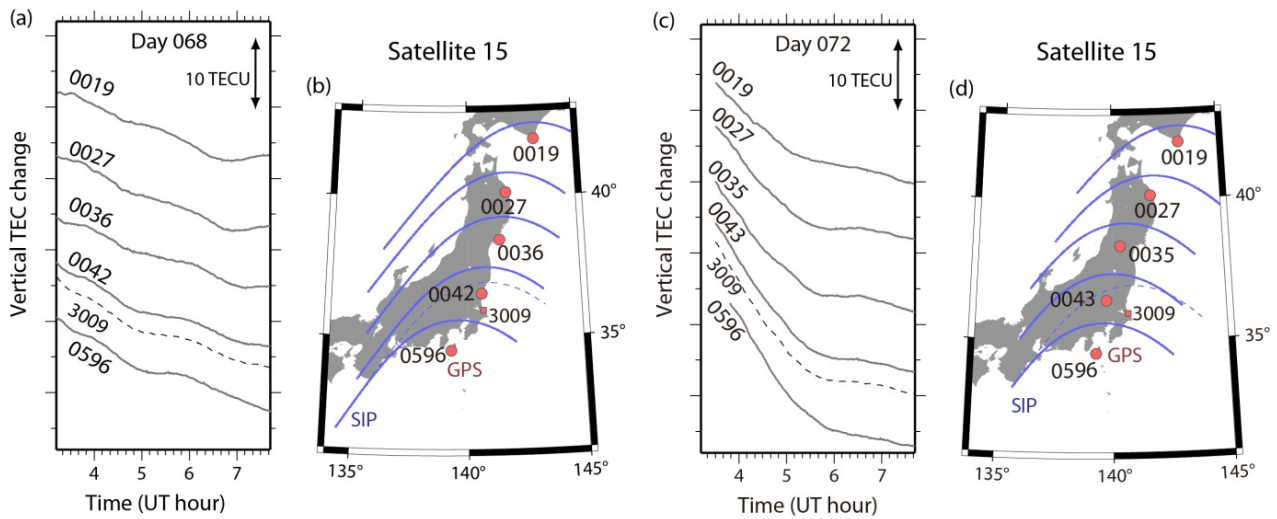
437
438
439 Figure A4. The VTEC data of Satellite 15 at 3009 plotted in Figure 6d sometimes show rather sharp variations. We
440 picked up the two cases (shown by reverse triangles in Figure 6d), and their propagation properties are shown here.
441 (a) VTEC time series at 3009 (broken curve) on the day 068 show a local minimum at ~5 UT and maximum at ~6 UT.
442 Such minima and maxima are seen in other GPS stations, and the occurrence time differs by ~0.5 hour between the
443 northernmost and the southernmost GPS stations. This corresponds to the propagation speed of ~0.3 km/s, and
444 suggests that this is a small amplitude LSTID coming from the auroral oval. The SIP trajectory and the GPS site
445 positions are shown in (b). In (c, d), we show that another sharp bend of ~5.5 UT at 3009 is also a part of LSTID
446 propagating southward.
447